

# Characteristics of the Irradiated Hamamatsu p-Bulk Silicon Microstrip Sensors

K. Hara, H. Hatano, T. Meguro, S. Mitsui, T. Okuyama, M. Yamada, Y. Ikegami, T. Kohriki, S. Terada, Y. Unno, K. Yamamura, and S. Kamada

**Abstract**—Microstrip silicon sensors with p-bulk and n-readout are investigated as a radiation hard device for the Super LHC experiment. We evaluated the radiation hardness of the sensors fabricated by Hamamatsu Photonics through irradiation with 70-MeV protons up to the fluence of  $5 \times 10^{15}$  1-MeV  $n_{eq}/cm^2$  and with  $^{60}Co$   $\gamma$ s at a rate foreseen at the Super LHC. The strip isolation and punch-through properties are characterized in detail. Various strip isolation structures, p-stop, p-spray and both combined, are examined. The results are compared among commercially available MCZ and two types of FZ wafers.

## I. INTRODUCTION

DEVELOPMENT of radiation hard silicon microstrip sensors is essential for the future high luminosity experiments such as at the Super LHC where the radiation environment will be ten-fold increased compared to the LHC, the total fluence reaching  $1 \times 10^{15}$  1-MeV  $n_{eq}/cm^2$  [1]. High resistive n-type FZ silicon is known to invert after receiving a fluence of a few  $\times 10^{13}$  n/cm<sup>2</sup>. The lifetime of the present LHC ATLAS microstrip sensors, p<sup>+</sup>-on-n sensors, is determined by the full depletion voltage increase when it exceeds the voltage limit of the system. As a candidate of radiation hard microstrip sensors for the Super LHC, we are investigating p-type bulk sensors, n<sup>+</sup>-on-p sensors [2]. In such devices, the junctions stay at the strip side throughout the lifetime, allowing the signals to be read out even at reduced bias once the full depletion voltage reached the applicable limit. Sufficient charge collection is possible [2], [3] even after irradiation owing to the high electron mobility that helps reduce the probability of carries being trapped.

The microstrip sensors constructed at large scale have employed so far n-type wafers [4]. In p-type wafers, positive charges inherently trapped in the oxide layer accumulate a layer of mobile electrons in the silicon surface between the readout strips, which may prevent their independent operation. Availability of high quality p-bulk wafers has been also an issue. High resistive p-bulk MCZ (magnetic Czochralski) wafers became available recently and are less costly than FZ

(float zone) wafers. We have fabricated p-bulk microstrip sensors adopting technologies such as p-stop and p-spray for strip isolation. Since the strip isolation concerns surface conditions, the evaluation should be made on the sensors fabricated from commercially available wafers and by one of the companies capable of mass production, e.g., Hamamatsu Photonics.

Our R&D fabrication has been made in three periods, referred to ATLAS05, 06 and 07. The first ATLAS05 was processed with a Hamamatsu 4" technology and using FZ and MCZ wafers. ATLAS06 was completed with a Hamamatsu 6" using FZ and MCZ wafers, including FZp wafers where the defects are fewer than in normal FZ. A series of general characterization measurements of these samples, both non-irradiated and irradiated, is reported elsewhere [2]. ATLAS07 process is currently carried out in a wider collaboration [5] where FZp wafer is selected. In this paper, we report new measurements on the annealing property of ATLAS06 samples, and punch-through (PT) evaluated on ATLAS06 test structures. The PT property of PT implemented ATLAS07 is also described. These samples were irradiated with 70-MeV protons up to a fluence of  $5 \times 10^{15}$  1-MeV  $n_{eq}/cm^2$ . The strip isolation and PT properties are also evaluated while irradiated with  $^{60}Co$   $\gamma$ 's at a similar rate foreseen at the Super LHC.

## II. SAMPLES AND IRRADIATION

The sample sensors are 1 cm  $\times$  1 cm in area and 300  $\mu$ m in thickness. The strip pitch is 80  $\mu$ m for ATLAS05 and 06, and 74.5  $\mu$ m for ATLAS07. The wafer types, and p-stop and p-spray concentrations are summarized in Table I. The crystal orientation is <111> only for 4" FZ; others are <100>. Various strip isolation structures have been examined including AC and DC field plates [2], but it turned out that they are not

TABLE I  
THE SAMPLES FOR THE THREE PROCESSES. FZ IS FLOAT ZONE (FZP HAS FEWER DEFECTS) AND MCZ IS MAGNETIC CZOCHRALSKI. LISTED ARE CRYSTAL ORIENTATION, P-STOP AND P-SPRAY CONCENTRATIONS IN /cm<sup>2</sup>. THE CONCENTRATION VALUES ARE INDICATIVE ONLY.

Process	wafers	P-stop HI [cm <sup>-2</sup> ]	P-stop LO/Mid [cm <sup>-2</sup> ]	P-spray (P-stop)
ATLAS05	FZ/MCZ	$20 \times 10^{12}$	$5 \times 10^{12}$	$2 \times 10^{12}$
HPK4"	<111>/<100>			$(2 \times 10^{12})$
ATLAS06	FZp/FZ/MCZ	$20 \times 10^{12}$	$10 \times 10^{12}$	$2 \times 10^{12}$
HPK6"	<100>			$(8 \times 10^{12})$
ATLAS07	FZp	n/a	$10 \times 10^{12}$	$2 \times 10^{12}$
HPK6"	<100>			$(8 \times 10^{12})$

Manuscript received November 14, 2008. This research was partially supported by the Ministry of Education, Science, Sports and Culture, Grant-in-Aid for Scientific Research A20244038, 2008 and C20540291, 2008

K. Hara (e-mail: hara@hep.px.tsukuba.ac.jp), H. Hatano, T. Meguro, S. Mitsui, T. Okuyama (now at University of Tokyo), M. Yamada are with the Institute of Pure and Applied Sciences, University of Tsukuba, Tsukuba, Ibaraki 305-8571, Japan.

K. Ikegami, T. Kohriki, S. Terada and Y. Unno are with the IPNS, High Energy Accelerator Research Organization, KEK, Tsukuba, Ibaraki 305-0801, Japan.

K. Yamamura, and S. Kamada are with Solid State Division, Hamamatsu Photonics K.K., Hamamatsu, Shizuoka 435-8558, Japan.

effective and only conventional p-stop structures, common and individual, survived in ATLAS07. A common p-stop (called Z3) is the isolation structure mainly discussed in this paper. No structure (Z1) is also examined. P-spray at a fixed concentration of  $2 \times 10^{12}/\text{cm}^2$  is added to some of Z1 and Z3 samples. Hence, Z1 with p-spray represents the performance of the p-spray only. As shown in the table, the p-stop concentration of p-spray samples is a half of HI p-stop concentration.

The PT characteristics is first studied with test structures of ATLAS06, and implemented in ATLAS07 where the distance between the implant end to the bias-ring is set to 12  $\mu\text{m}$ . In ATLAS07, Z3 with a distance of 70  $\mu\text{m}$  is also fabricated for comparison. They are referred to ATLAS07-Z1(PT), Z3(PT) and Z3, respectively.<sup>1</sup>

The proton irradiation was carried out using 70-MeV protons of CYRIC, Tohoku University. The details of the irradiation and fluence calibration are described elsewhere [2]. During the irradiation the samples were biased at 100 V and cooled to  $-10^\circ\text{C}$ . The irradiation took typically a few 10 min to a few hours, depending on the total fluence. The irradiated sensors were kept refrigerated throughout except that they were placed at  $60^\circ\text{C}$  for 80 min to complete the initial annealing. Some samples were characterized during this process and in extended period to study the annealing property.

The cobalt irradiation was made at Takasaki Laboratory of JAEA. The isolation and PT properties are primarily concerned to the surface conditions, e.g., the charge accumulation in the oxide. Such an effect can be evaluated by ionization radiation by  $^{60}\text{Co}$   $\gamma$ 's as well. The dose rate was targeted to exceed the expected maximum fluence at the Super LHC. The ATLAS values [6] multiplied by 10 are 7.59 kGy annually ( $10^7$  s) and  $1.5 \times 10^7$  charged particles/ $\text{cm}^2$ 's at the radius of 30 cm. If the charged particles are treated as minimum ionizing, this results in 15 Gy/h or 3 Gy/h for the average. Taking a safety factor into account for the soft particle contribution and the fact that we evaluate on 1 cm square samples with respect to 10 cm square real sensors where the surface charge may harder to move in the direction along the strips, we set the initial dose rate to 100 Gy/h. The irradiation at 100 Gy/h continued for 22 h. After a break for 0.5 h, the test was extended at 1 kGy/h for 5 h.

In total 16 samples were irradiated together with  $^{60}\text{Co}$ , see Table II. For three types of ATLAS06 wafers, FZp, FZ and MCZ, we tested Z1 with and without p-spray, and Z3 (with HI p-stop) with and without additional p-spray. For ATLAS07 (FZp), Z3 and Z3(PT) with and without p-spray were irradiated. The characterization was repeated every hour, starting with I-V and isolation measurements up to 450 V bias, and then PT measurement at a fixed bias of 300 V. The  $^{60}\text{Co}$  source was in place during the characterization. The bias voltage between characterization measurements was kept at 300 V, except for the last one hour at 1 kGy/h where the bias was raised to 450 V. The biases were provided by a single source meter with 100 k $\Omega$  resistors inserted to individual

samples. The detector leakage current was evaluated in turn by measuring the voltage drop across the resistor with Keithley 2400. Two DC pads at neighbor were wire-bonded per sample and the contacts were extracted outside the irradiation cave using 12 m long twisted pair cables. One pair selected with relays at a time were measured on the isolation between and one of the two against the ground (bias-ring) for PT measurement. We relied on the dose rate based on the calibration provided by the irradiation facility (15 and 55 cm from the source for 1 kGy/h and 100 Gy/h exposures, respectively). The induced current seen by the sensors under test was checked to be consistent with the value expected from the nominal irradiation rate. The irradiation was made at room temperature.

TABLE II  
16 SAMPLES IRRADIATED WITH  $^{60}\text{Co}$   $\gamma$ 's. ATLAS06 P-STOP ONLY SAMPLES ARE HI DENSITY

PROCESS	WAFER	NONE	P-STOP ONLY	+SPRAY
ATLAS06	FZ	Z1, Z3	Z3 (HI)	Z1, Z3
	MCZ	Z1	Z3 (HI)	Z1, Z3
	FZp	Z1	Z3 (HI)	Z1, Z3
ATLAS07	FZp		Z3, Z3(PT)	Z3, Z3(PT)

### III. RESULTS

#### A. Isolation: proton irradiated samples

The strips are electrically isolated at bias voltages sufficiently high to remove the electron accumulation between the strips. We characterized the isolation by applying fixed voltages (+5V and -5V) between a pair of the DC pads and measuring the induced current, while changing the bias voltage. The induced current is determined by the total resistance, sum of two bias resistors in series and interstrip resistance parallel to them. Fig. 1 summarizes the isolation of proton irradiated ATLAS06 samples for various isolation structures, Z1 to Z4 [2]. The isolation voltage is defined by the bias voltage where the measured current reaches the asymptotic value within 10% deviation. The nine graphs correspond to the three wafer types, and two p-stop concentrations (H and M) and p-spray in addition (P).

In each group, the curves are notably different for no p-stop structure (Z1) and others (Z2 to Z4). The isolation voltage of Z1 samples is low for small fluences below  $\sim 5 \times 10^{14}$  n/ $\text{cm}^2$  for FZp wafers and samples with p-spray. FZp wafers which have fewer defects behave better in isolation property than the others at low fluence, but addition of p-spray to the other wafers improves to a similar level. For a fluence exceeding  $\sim 1 \times 10^{15}$  n/ $\text{cm}^2$ , only the p-stop samples with high concentration (HI) exhibit small isolation voltages. In general, however, the isolation is achievable below the operation voltage, typically 300 V, for all the samples.

<sup>1</sup> The zone structures are detailed in [2] for ATLAS05 and 06. For ATLAS07 process, Z3 and Z3(PT) here are named Z4 and Z3, respectively.

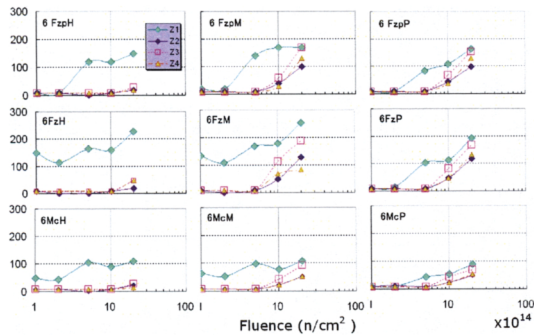


Fig. 1. Strip isolation voltages [V] as a function of fluence, shown for 6'' Fz with fewer defects (FzP, upper), standard FZ (FZ, middle) and MCZ (Mc, lower). Results for four p-stop structures are shown, where Z1 has no structure (H and M), or has p-spray only (P).

### B. Isolation under continuous <sup>60</sup>Co irradiation

The isolation described above was evaluated after the annealing was completed. The annealing time, however, concerns the recovery of the bulk damages and may not be appropriate for the surface damages. The isolation and PT properties are primarily related to the latter.

We carried out in-situ evaluation of the isolation and PT under <sup>60</sup>Co irradiation. The characterization of isolation is the same as described before, measure the induced current applying +5 V and -5 V to one of the DC pads while the other DC pad at neighbor at ground. Two voltage results were compared to cross check the measurements: We obtained consistent results from the two. The resistance corresponds to the two bias resistors in series of about 2.5 MΩ if no significant contribution of the interstrip resistance is present. Fig. 2 shows a typical set of data, taken after 15 h irradiation at 100 Gy/h. Out of 16 samples, MCZ Z1 sample with p-spray was disconnected from the system, since it showed a large leakage current shortly after the irradiation started.

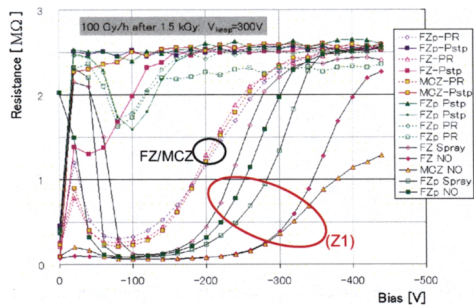


Fig. 2. Typical set of R-V curves for the isolation measurement, shown for 15 samples. This set is taken after 15 h at 100 Gy/h. PR refers to Z3 p-stop and p-spray, Pstp to Z3 HI p-stop, Spray and NO refer to Z1 with and without p-spray, respectively.

The data at bias voltages below the full depletion show additional components, but the data above 100 V are consistent that the isolation is achieved as the voltage is raised.

The curves can be grouped into three. All tested Z1 (FZp and FZ with and without p-spray, and MCZ without p-spray) samples showed most degraded characteristics among these. The second group is FZ and MCZ samples where the p-spray is applied (the p-stop concentration is Mid); FZ and MCZ samples with HI p-stop and ATLAS07 are in the third group which showed a most preferable characteristics. The sensors in the first group should exhibit substantial cross talks since the bias was kept at 300 V. This needs to be verified with sensors with readout connected.

The wafer difference is summarized in Fig. 3 where the isolation voltages are averaged over Z3 samples. Here ATLAS07 (FZp) data are shown separately. For all the wafers, the isolation voltage starts increasing at around 1 kGy accumulated dose. The break 0.5 h while switching to 1 kGy/h contributed to lower the isolation voltage. The bias voltage during the irradiation was 300 V except for the last one hour where the bias was 450 V.

The curves for FZp wafer are shown individually in Fig. 4 including Z1 samples. The HI p-stop and ATLAS07 Mid p-stop behaved better in the 22 h exposure at 100 Gy/h. These two samples also increased gradually at 1 kGy/h exposure. As mentioned before, both Z1 samples behaved worse than the others.

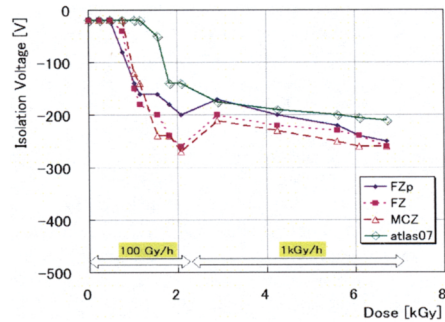


Fig. 3. The isolation voltage averaged for Z3 samples as a function of accumulated dose.

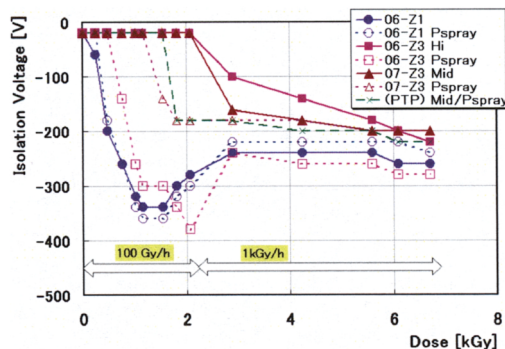


Fig. 4. The isolation voltages for FZp samples. The samples with p-spray are shown in dotted curves with open marks. Two ATLAS07 Z3(PTP) samples, with Mid p-stop and p-spray, are overlapped each other, shown in crosses.

Exposure at 1 kGy/h was made to evaluate if the isolation is completely lost at such a high rate or not. The both sets of data indicate that the isolation degradation has a time constant probably independent to the radiation rate. It is reported [7] that Hamamatsu n-bulk sensors for the ATLAS SCT show degrade strip isolation when the bias voltage is lowered after a substantial period of operation even if they are not exposed to any radiation. The explanation is that holes created in a long time operation are arranged such that the isolation is achieved at the voltage a few 10 V below the operation voltage. Once the voltage is lowered, holes start to re-arrange to fit in the new field. The isolation turns to be degraded during this rearrangement. Since the mobility of holes in the oxide is small, the re-arrangement takes days to weeks especially at low temperature. The present situation under  $^{60}\text{Co}$  irradiation may be similar. Unless the isolation is completely lost by the radiation induced current, the isolation voltages may be sustained to be slightly smaller than the operation voltage. Examination using real size sensors with readout electronics connected is required in order to discuss such an effect qualitatively in terms of noise and charge collection performance.

### C. Punch through

In a rare case of accelerator beam loss spraying around the core of the beam, the silicon detector may receive intensive flux of protons. If the signal current boosts up the implant voltage too large with respect to the oxide voltage rating, the oxide will be broken, resulting the particular channel and most likely some neighbors to become noisy, or in worst case the whole sensor will be permanently damaged. Such a large voltage could present due to the finite resistance of the bias resistor (about 1.5 M $\Omega$ ) and also of the implant resistance [8]. The punch through (PT) between the  $n^+$  strip end to the bias-ring ( $n^+$ ) can lower the risk against such beam splash if it occurs at a voltage smaller than the oxide rating 100 V.

We irradiated ATLAS06 test structures where the distance between  $n^+$  implants was varied to 8, 12 and 20  $\mu\text{m}$ . Structures with a  $p^+$  implant interleaving between are also examined, simulating the p-stop structure surrounding the strip. The structures are named either  $nG$  or  $nCG$ , where  $n$  denotes the distance in  $\mu\text{m}$ , C is with a p-stop electrode between. The PT characteristics is evaluated by changing the test voltage applied to one of the electrodes, and measuring the induced current across. The data were taken for a set of bias voltages. The induced current increases linearly with the test voltage for small voltages, corresponding to the bias resistance, and becomes larger at higher voltages when the PT is turned on. The turn-on voltage is defined as the test voltage where the measured resistance between the electrodes dropped to 500 k $\Omega$ . A typical set of data are plotted in Fig. 5 for non-irradiated and two proton irradiated FZ samples. The 400 V data for MCZ, where the deviation was the largest are also plotted as a comparison. The difference is not large among different wafer types and p-sprayed or not. A distance of 8  $\mu\text{m}$  is too close for small PT voltages at pre-irradiation and  $\sim 6 \times 10^{14}$   $\text{n}/\text{cm}^2$ , while 12  $\mu\text{m}$  and 20  $\mu\text{m}$  seem to be appropriate. It is shown that the irradiation will reduce the PT voltages.

The PT structure is implemented in ATLAS07 where a distance of 12  $\mu\text{m}$  was chosen. They are named Z1(PT) and Z3(PT). Z3 with a distance of 70  $\mu\text{m}$  is also included for comparison.

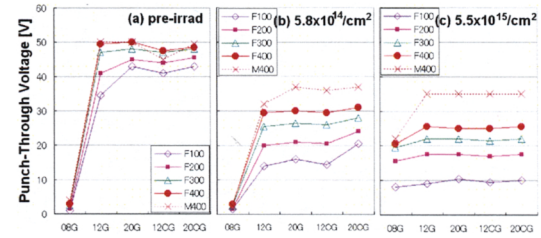


Fig. 5. The punch-through voltages for non-irradiated and samples irradiated with protons to two fluence values. The horizontal is the gap distance between the ends of two  $n^+$  strips with (C) or without a  $p^+$  electrode between. The data are at different bias voltages from 100 V (diamonds) to 400 V (circles) for standard FZ, and at 400 V for MCZ.

Fig. 6 shows the measured current in the PT evaluation for the samples irradiated with protons to  $2.1 \times 10^{14}$  and  $2.3 \times 10^{15}$   $\text{n}/\text{cm}^2$ . The test voltage was applied to the DC pad while the bias-ring set at the ground, with the bias fixed at 300 V. The data are compared between Z1(PT), Z3(PT) and Z3 from ATLAS07, with and without p-spray. The Z1 samples show a simple PT characteristics with PT taking place below 20 V in the negative voltage range. The shape is slightly disturbed if p-spray is added. In the positive range, the PT voltage increases with radiation and was not observed below 100 V for the  $1.3 \times 10^{15}$   $\text{n}/\text{cm}^2$  sample. The positively charged oxide layer helps to lower the PT voltage in the negative region, as seen in the test structure, which in turn prohibits the PT to occur in the test structure. Since the beam splash produces negative current, PT should turn on in such a case. The PT of Z3(PT) takes place in two steps, first gradually with the test voltage and suddenly at some voltage. Such a behavior was not seen in the test structure. The PT occurrence is prohibited in the sample most probably due to that the common p-stop is by far solid due to a larger total area compared in the test structure.

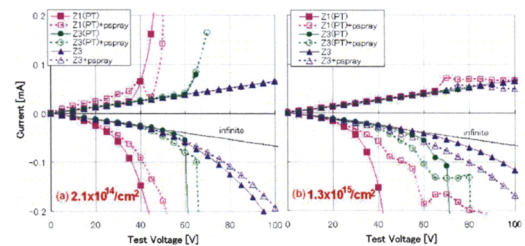


Fig. 6. The induced current as a function of the test voltage (punch-through measurement) after (a)  $2.1 \times 10^{14}$   $\text{n}/\text{cm}^2$  and (b)  $1.3 \times 10^{15}$   $\text{n}/\text{cm}^2$ . The samples are ATLAS07 (FZp) with (squares) Z1(PT), (circles) Z3(PT) and (triangles) Z3. Samples with p-spray are shown in open marks and dotted curves. The bias voltage is 300 V. The line labeled "infinite" in the negative side corresponds to the case where no PT takes place.

Fig. 7 is an evolution of R-V curves with time showing the data before irradiation, after 1 h at 100 Gy/h, after 22 h at 100 Gy/h, and after additional irradiation of 5 h at 1 kGy/h. The data were taken while irradiated and with a bias of 300 V. The PT characteristics became similar for the two samples, although they showed different initially.

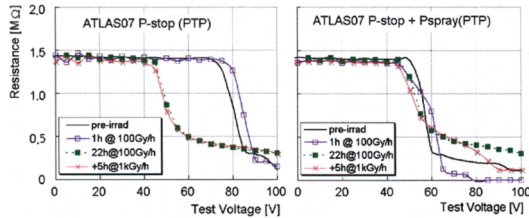


Fig. 7. The strip to bias-ring resistance as a function of the test voltage for Z3(PT) samples (left) without and (right) with p-spray. The data are measured while irradiated with  $^{60}\text{Co}$  with the bias kept at 300 V.

#### D. Annealing

Studying the annealing of irradiated sensors is important for detector operation and maintenance points of view. For n-bulk sensors where the property is well studied, the effective impurity concentration decreases at first, and then increases. The time scale is dependent on the temperature. The minimum is at approximately 80 min at 60°C temperature.

The study is carried out for the p-bulk sensors irradiated to  $2 \times 10^{14} \text{ n/cm}^2$ . The full depletion voltage was evaluated both by C-V measurement and by charge collection measurement using an infrared laser. The results of the full depletion voltage evolution are summarized in Fig. 8. The p-bulk sensors are found to exhibit similar annealing property to n-bulk sensors. Among these, the MCZ shows a slightly quicker evolution with time, after the minimum is experienced. The strip isolation voltages were also measured, which showed to decrease monotonically with time.

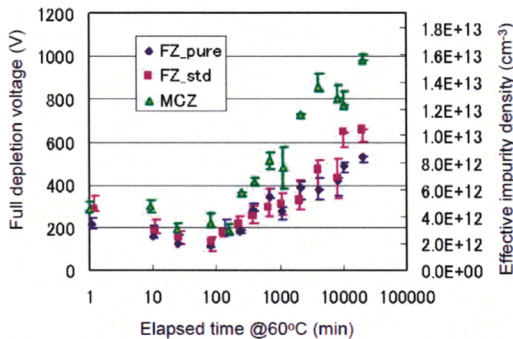


Fig. 8. The evolution of full depletion voltage as a function of elapsed time for the annealing temperature of 60°C. The data are shown for the three wafer types.

#### IV. SUMMARY

We have evaluated characteristics of Hamamatsu p-bulk microstrip sensors with emphasis on the strip isolation and

punch-through properties after proton irradiation and during a low dose rate  $^{60}\text{Co}$  irradiation. The results are compared between three types of wafers and p-stop and p-spray configurations. FZp wafers which have fewer defects than standard FZ are selected for the current sensor process ATLAS07.

The strip isolation is achieved reliably with p-stop of  $2 \times 10^{13} \text{ /cm}^2$  for proton irradiation exceeding  $10^{15} \text{ n/cm}^2$  and during  $^{60}\text{Co}$  irradiation at a level foreseen at the Super LHC. The strip isolation voltage increases under irradiation, reaching the value close to the operation voltage for the samples with lower density p-stop with or without p-spray. The influence of such increased isolation voltage to the detector performance needs to be examined with readout electronics connected through the achievable signal and noise figures.

The punch through protection was implemented in the ATLAS07 process. The punch through occurs at voltages higher than expected from the test structure for the samples where p-stop electrodes interleave between the  $n^+$  electrodes.

#### REFERENCES

- [1] I. Dawson, "Radiation background simulations and measurements for ATLAS at the SLHC", talk given at ATLAS Upgrade Workshop, Valencia, Dec 2007. The total dose is evaluated as  $0.9 \times 10^{15} \text{ n/cm}^2$  at the radius of 30 cm taking a safety factor of two for integrated luminosity of  $3000 \text{ fb}^{-1}$ .
- [2] K. Hara et al., "Development of Radiation Hard N-on-P Silicon Microstrip Sensors for Super LHC", IEEE 2007 Nuclear Science Symposium and Medical Imaging Conference, Conference Record N15-245, Oct. 27-Nov. 3, 2007, Honolulu, Hawaii.
- [3] G. Casse et al., "Response to minimum ionising particles of p-type substrate silicon microstrip detectors irradiated with neutrons to LHC upgrade doses", Nucl. Instr. Methods A581 (2007) 318; M. Minano et al., "Characterization of irradiated detectors fabricated on p-type silicon substrates for super-LHC", Nucl. Instr. Methods A583 (2007) 33.
- [4] LHCb VELO replacement employs n'-on-p sensors in part, see A. Affolder et al., "LHCb-VELO module production with n-side read-out on n- and p-type silicon substrates", Nucl. Instr. Methods A583 (2007) 18.
- [5] See, for example, Y. Unno, ATLAS Tracker Upgrade Meeting, Nov 3-7, 2008, NIKHEF, The Netherlands.
- [6] The ATLAS Collaboration, G. Aad et al. "The ATLAS Experiment at the CERN Large Hadron Collider", JINST 3 (2008) S08003.
- [7] Y. Nakamura et al., "Anomalous IV behavior of ATLAS SCT microstrip sensors", Nucl. Instr. Methods A575 (2007) 353.
- [8] K. Hara et al., "Beam splash effects on ATLAS silicon microstrip detectors evaluated using 1-W Nd:YAG laser", Nucl. Instr. Methods A541 (2005) 15.